

HIGH-FIDELITY PROGRESSIVE FAILURE ANALYSES OF COMPOSITE LAMINATES UNDER IMPACT LOADING

Z.C. Su¹, D.C. Pham², N. Sridhar³

¹Institute of High Performance Computing, A*STAR, 1 Fusionopolis Way, Singapore
Email: suzc@ihpc.a-star.edu.sg Web Page: <https://www.a-star.edu.sg/ihpc/People>

²Institute of High Performance Computing, A*STAR, 1 Fusionopolis Way, Singapore
Email: phamdc@ihpc.a-star.edu.sg Web Page: <https://www.a-star.edu.sg/ihpc/People>

³Institute of High Performance Computing, A*STAR, 1 Fusionopolis Way, Singapore
Email: narayanas@ihpc.a-star.edu.sg Web Page: <https://www.a-star.edu.sg/ihpc/People>

Keywords: progressive failure, composite laminates, low-velocity impact, delamination

Abstract

In this study, an effective approach for high-fidelity progressive failure analyses of composite laminates subjected to low-velocity impact is developed. Both in-plane progressive damage and interlaminar delamination are included. The in-plane damage initiation of different failure modes is triggered by the Hashin criteria and the following softening is assumed to be linear. The potential delamination between plies of different orientations is modeled using cohesive elements. The non-linear in-plane shear behavior before damage initiation is approximated by a third-order polynomial. This progressive damage model is implemented as user-defined material (VUMAT) subroutines in ABAQUS/Explicit. Finite element (FE) analyses of low-velocity impact on a cross-ply graphite/epoxy composite laminate ($[0_3/90_3]_s$) are performed. In the FE models, one layer of 3D continuum shell elements are employed to represent plies of the same orientation and one layer of cohesive elements are used to mimic the resin-rich interface between plies with different orientations. Comparing numerical results with experimental results from the existing literature, it is found that both the dynamic response and damage patterns are accurately predicted. Additional numerical analyses without shear non-linearity are also conducted to investigate its influence on dynamic response and damage patterns. The analyses show that proper incorporation of shear non-linearity is necessary.

1. Introduction

Carbon fiber composites have found increasing applications in light-weight structural members, in fields of aerospace, automobile and marine as they have high specific strength/stiffness, good corrosion resistance, and excellent fatigue performance. One limitation for wide application of composites is their vulnerability to impact loads which can result in significant loss in their load-carrying capacity. Understanding detailed failure mechanisms of composite laminates upon impact is challenging since multiple mechanisms can manifest including various types of intra- and inter-laminar damage such as fiber breakage, transverse matrix cracking, interlaminar delamination, etc. Besides, different failure mechanisms interact with each other making it more challenging to study the damage progression. Because of the complexity of damage mechanisms, development of effective computational models for impact damage characterization and analysis become critical. The computational methods are beneficial since they help reduce the costs of impact tests and associated damage verification and certification costs.

Recently, low-velocity impact on composite laminates of various stacking sequences and materials systems has been extensively studied both experimentally [1–4] and numerically [2, 4–7]. Most numerical studies utilize three dimensional (3D) solid elements to model composite plies. Normally, each lamina or ply is modeled by only one layer of 3D solid elements to reduce computational time. This simplification results in inaccurate modeling of bending in each ply. This issue may be solved by using three dimensional continuum shell elements, which can capture correct bending response and accurate through-thickness response for composite laminate structures.

This paper presents an effective approach for high-fidelity progressive failure analyses of composite laminates subjected to impact loading with different velocities/energies. The progressive damage model includes in-plane failure of composite plies and interlaminar delamination. The in-plane damage initiation is triggered by Hashin criteria and the damage progression is modeled by a smeared crack model which employs energy-based linear softening laws for different failure modes. The potential delamination is modeled by cohesive elements. Moreover, the non-linear shear behavior of composite materials observed in experiments [2, 7] is also included in this model. It is approximated by a third-order polynomial before damage initiation.

The proposed progressive damage model is employed to study the dynamic responses and damage progression of a cross-ply ($[0_3/90_3]_s$) graphite/epoxy plate subjected to impact loading. Finite element (FE) analyses are performed with ABAQUS/Explicit, and user defined subroutines (VUMAT) are developed for implementing the proposed progressive damage model. In the FE models, one layer of 3D continuum shell elements are employed to model the composite plies with the same orientation and one layer of cohesive elements are used to represent the interface between the plies with different orientations. Compared to commonly used FE models with 3D solid elements, the computational time can be significantly reduced enabling us to carry out comprehensive studies on damage progression in composite laminates subjected to impact loading. FE simulations show that the the model developed in this study can accurately predict impact force and damage patterns for different impact energies. Another type of FE models without non-linear shear behavior are also developed to examine the necessity of modeling non-linear shear behavior. It is seen that the progressive damage model with shear non-linearity predicts more accurate dynamic response and damage patterns than the model without shear non-linearity does.

2. Failure theory

The failure theory employed here follows a previous study by Su et al. [8], which includes in-plane failure of composite plies and delamination at interfaces between plies of different orientations. The theory is briefly summarized here.

2.1. Modeling in-plane failure

Hashin failure criteria [9] are employed to determine in-plane damage initiation and the post-failure softening behavior is assumed to be linear.

Hashin criteria consist of four criteria for different damage modes including tensile fiber failure, compressive fiber failure, tensile matrix failure and compressive matrix failure [9]. Hashin criteria for the two dimensional case are given as,

Tensile fiber failure

$$\frac{\sigma_{11}}{X_t} = 1, \quad \sigma_{11} > 0 \quad (1)$$

Compressive fiber failure

$$\frac{\sigma_{11}}{X_c} = -1, \quad \sigma_{11} < 0 \quad (2)$$

Tensile matrix failure

$$\left(\frac{\sigma_{22}}{Y_t}\right)^2 + \left(\frac{\tau_{12}}{S_{12}}\right)^2 = 1, \quad \sigma_{22} > 0 \quad (3)$$

Compressive matrix failure

$$\left[\left(\frac{Y_c}{2S_{23}}\right)^2 - 1\right] \frac{\sigma_{22}}{Y_c} + \left(\frac{\sigma_{22}}{2S_{23}}\right)^2 + \left(\frac{\tau_{12}}{S_{12}}\right)^2 = 1, \quad \sigma_{22} < 0 \quad (4)$$

where σ_{11} and σ_{22} are stresses in fiber direction and transverse direction, respectively. τ_{12} is in-plane shear stress. X and Y denote the strengths in fiber and transverse directions with the subscripts t and c indicating tension and compression, respectively. S_{12} and S_{23} are shear strengths in 1-2 and 2-3 planes.

Subsequently, the smeared crack model, developed by Pinho et al. [10, 11], is employed to model damage propagation. For the fiber direction, the smeared crack model gives,

$$\int \sigma_{11} d(\epsilon_{11} l_c) = G_{fc} \quad (5)$$

where ϵ_{11} is the strain in fiber direction, l_c is the element characteristic length, and G_{fc} is translamellar fracture toughness. For a given element, l_c can be assumed to be constant. Therefore, Eq. 5 describes a bilinear relationship between stress and strain.

Transverse failure modes include both normal and shear components. Hence they are actually mixed-mode damage. To define a mixed linear softening law, equivalent stress and displacement are determined first. For transverse tensile failure, the fracture surface is usually normal to the transverse direction. Therefore, the equivalent stress and displacement can be defined as,

$$\sigma_{eq} = \sqrt{\sigma_{22}^2 + \tau_{12}^2}, \quad \delta_{eq} = \frac{2(G_N + G_S)}{\sigma_{eq}} \text{ with } G_N = \frac{1}{2} \langle \sigma_{22} \epsilon_{22} \rangle_+, \quad G_S = \frac{1}{2} \tau_{12} \gamma_{12} l_c \quad (6)$$

The linear softening law based on the energy criterion is then given as,

$$\int \sigma_{eq} d(\delta_{eq}) = G_{mc} \quad (7)$$

where G_{mc} denotes mixed-mode fracture energy, which can be calculated using the B-K formula,

$$G_{mc} = G_{nc} + (G_{sc} - G_{nc}) B^\eta, \quad B = \frac{G_S}{G_N + G_S} \quad (8)$$

where G_{nc} and G_{sc} are the normal and shear fracture toughnesses. η is a material parameter.

For transverse compressive failure, the fracture plane is normally an angle (ϕ) to the out-of-plane normal as illustrated in Fig. 1. ϕ is found to be around 53° for commonly used carbon-epoxy systems [11]. The shear stresses and shear strains in the fracture plane are given as,

$$\tau_T = -\frac{\sigma_{22}}{2} \sin(2\phi), \quad \tau_L = \tau_{12} \cos(\phi) \text{ and } \gamma_T = -\frac{\epsilon_{22}}{2} \sin(2\phi), \quad \gamma_L = \gamma_{12} \cos(\phi) \quad (9)$$

The equivalent stress and displacement can then be defined as,

$$\tau_{eq} = \sqrt{\tau_T^2 + \tau_L^2}, \quad \delta_{eq} = \frac{\tau_T \gamma_T + \tau_L \gamma_L}{\tau_{eq}} \quad (10)$$

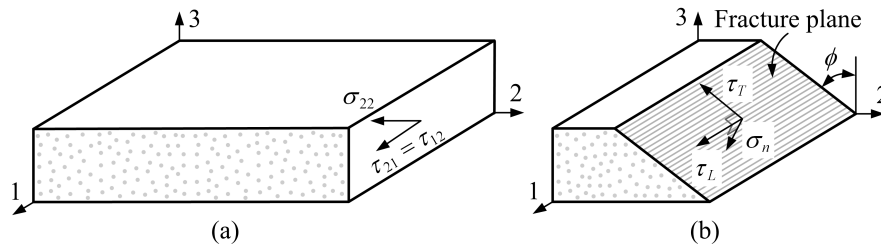


Figure 1. (a): Stress status of an element under in-plane shear and transverse compression; (b): Fracture plane and resolved stress components.

Hence, the linear softening law for transverse compression can be defined as,

$$\int \tau_{eq} d(\delta_{eq}) = G_{sc} \quad (11)$$

In previous study, the in-plane shear behavior of the composite is assumed to be linear elastic before damage initiation [8]. However, most composite materials exhibit non-linear shear behavior which are experimentally observed [2, 7]. In this study, the non-linear shear behavior is incorporated into the model through a third-order polynomial stress-strain curve,

$$\tau_{12} = c_1 \gamma_{12} + c_2 \gamma_{12}^2 + c_3 \gamma_{12}^3 \quad (12)$$

where c_1 , c_2 , and c_3 are coefficients fitting the shear stress-strain data from experiments [2, 7].

2.2. Interfacial delamination

The potential interfacial delamination is modeled using a cohesive element model with bilinear traction-separation laws. The initiation of delamination is assumed [12],

$$\frac{\langle t_n \rangle_+^2}{\sigma_n^c{}^2} + \frac{t_s^2}{\sigma_s^c{}^2} + \frac{t_t^2}{\sigma_t^c{}^2} = 1 \quad (13)$$

where t_n , t_s , and t_t denote the normal and shear tractions, and σ_n^c , σ_s^c and σ_t^c are the interfacial normal and shear strengths for the cohesive elements. Interfacial delamination is then modeled by the mixed-mode bilinear traction-separation law defined as,

$$\int T d\delta = G_{if} \quad (14)$$

where G_{if} is the mixed-mode fracture energy. T and δ are the equivalent quantities defined as,

$$T = \sqrt{\langle t_n \rangle_+^2 + t_s^2 + t_t^2}, \quad \delta = \sqrt{\langle \delta_n \rangle_+^2 + \delta_s^2 + \delta_t^2} \quad (15)$$

in which δ_n , δ_s , and δ_t are the relative displacements along the normal and two shear directions.

3. Finite element modeling

The progressive damage model is implemented in ABAQUS/Explicit through user-defined material (VUMAT) subroutines. Then a finite element model is developed to predict the impact response of a cross-ply composite laminate with the stacking sequence $[0_3/90_3]_s$, and the results are validated against experimental results from the existing literature.

The finite element model developed here represents the same setting-up in the experiments by Aymerich et al. [3, 5, 6]. As shown in Fig. 2, the finite element model is composed of three layers of continuum shell elements (SC8R) representing composite plies of different orientations and two layers of zero-thickness cohesive elements (COH3D8) between them representing the interfaces. The size of the plate is 87.5 mm × 65 mm × 2 mm. The hemispherical impactor of 12.5 mm in diameter and 2.3 kg in mass is modeled as a discrete rigid body. The supporting plate with a 67.5 mm × 45 mm rectangular opening is also modeled as a discrete rigid body and fixed to represent experimental constraints. Four spring elements at the four corners are used to represent the rubber clamps employed in experiments. Initial velocity is applied to the impactor through a predefined field in ABAQUS. Contact interaction is applied between the composite plate and the impactor with tangential friction (friction coefficient $\mu = 0.3$). The same interaction is defined between the rigid supporting plate and the composite plate. The material

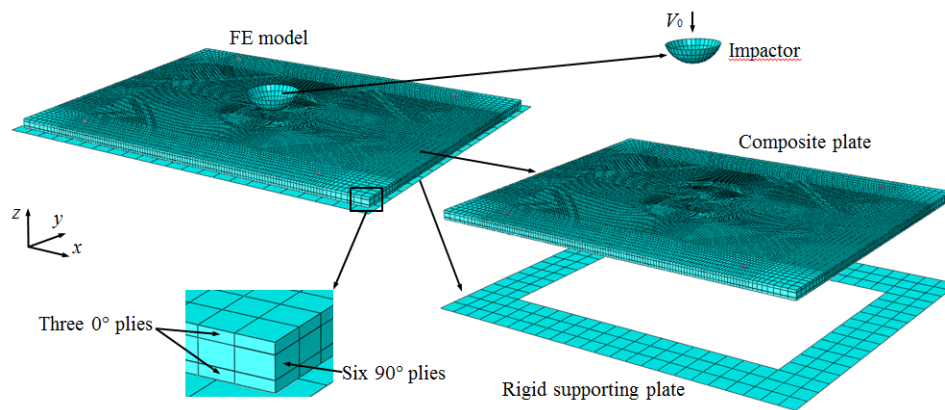


Figure 2. FE model for low-velocity impact analyses.

system employed in the experiments was HS160/REM graphite/epoxy. The properties for this material system are extracted from the existing literature [6, 7, 13] and are given in Table 1. Some properties are assumed based on the properties of similar material systems.

Table 1. Material properties.

Lamina properties	$E_{11} = 109.0 \text{ GPa}; E_{22} = 8.819 \text{ GPa};$ $G_{12} = 4.315 \text{ GPa}; G_{23} = 3.2 \text{ GPa};$ $X_t = 1850 \text{ MPa}; X_c = 1470 \text{ MPa};$ $Y_t = 40 \text{ MPa}; Y_c = 140 \text{ MPa};$ $S_{12} = 60 \text{ MPa}; S_{23} = 90 \text{ MPa};$ $G_{fc}^t = 92 \text{ kJ/m}^2; G_{fc}^c = 80 \text{ kJ/m}^2;$ $G_{nc} = 0.52 \text{ kJ/m}^2; G_{sc} = 0.97 \text{ kJ/m}^2;$ $\nu_{12} = 0.342; \eta = 1.45;$ $c_1 = 6.45 \text{ GPa}; c_2 = -156.8 \text{ GPa}; c_3 = 1415.7 \text{ GPa}$
Interface properties	$K_N = 120 \text{ GPa}; K_S = K_T = 43 \text{ GPa};$ $N = 30 \text{ MPa}; S = T = 80 \text{ MPa};$ $G_{Ic} = 0.52 \text{ kJ/m}^2; G_{IIc} = G_{IIIc} = 0.97 \text{ kJ/m}^2$

4. Results and discussions

FE analyses are performed, and the results are examined and compared with those obtained from experiments done by Aymerich et al. [3]. FE analyses without shear non-linearity are also performed to manifest the importance of including non-linear in-plane shear behavior in the progressive damage modeling.

4.1. Dynamic response

The impact force time histories from the FE analyses with and without in-plane shear non-linearity are compared with those obtained from experiments by Aymerich et al. [3, 5]. Fig. 3 shows the comparison of impact force time histories for impact energies 2.1 J and 5.1 J. As can be seen, the numerical results predicted from the model with shear non-linearity agree well with experimental results in terms of both impact duration and maximum impact force. However, the FE model without shear non-linearity predicts slightly larger impact duration and lower impact force before reaching the maximum compared with experimental results. This is mainly because that the model without shear non-linearity predicts earlier damage initiation in transverse direction and more extensive damage propagation thereafter than the experiments.

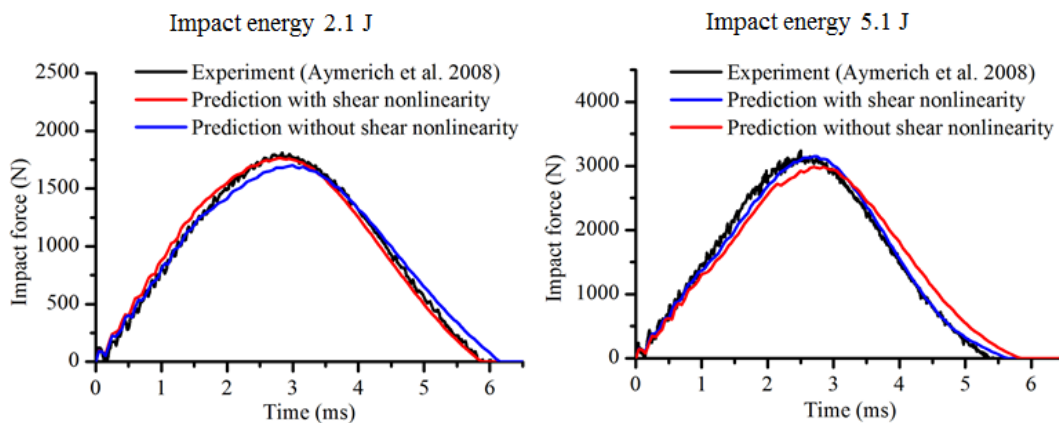


Figure 3. Comparison of impact force time histories between FE simulations and experiments.

4.2. Damage patterns

The major damage mechanisms are the peanut shape delamination at the bottom $90^\circ/0^\circ$ interface as shown in Figs. 4 and 5 (Red indicates fully delaminated region), and the bending matrix cracking in the bottom 0° plies as shown in Figs. 6 and 7 (Red indicates fully cracked region). In general, the damage patterns predicted by the model with shear non-linearity agree better with the experiments than those obtained from the model without shear non-linearity. It should be noted that numerical instability occurs for the model without shear non-linearity when the impact energy is relatively high as indicated in Fig. 7 (c), which shows abnormal matrix cracking for impact energy 5.1 J.

5. Conclusion

A high-fidelity progressive damage model was developed to study impact responses of a cross-ply ($[0_3/90_3]_s$) graphite/epoxy composite laminate under different impact energies. Both in-plane progres-

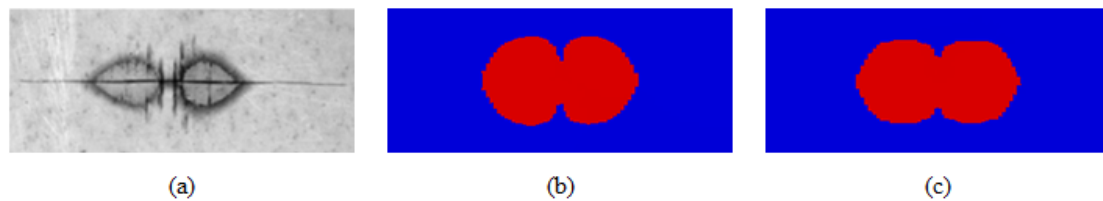


Figure 4. Delamination at the lower $90^\circ/0^\circ$ interface (impact energy 2.1 J): (a) Experiment [5], (b) Prediction with shear non-linearity, and (c) Prediction without shear non-linearity.

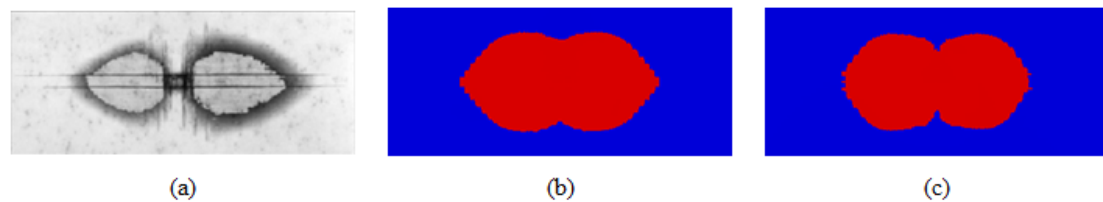


Figure 5. Delamination at the lower $90^\circ/0^\circ$ interface (impact energy 5.1 J): (a) Experiment [5], (b) Prediction with shear non-linearity, and (c) Prediction without shear non-linearity.

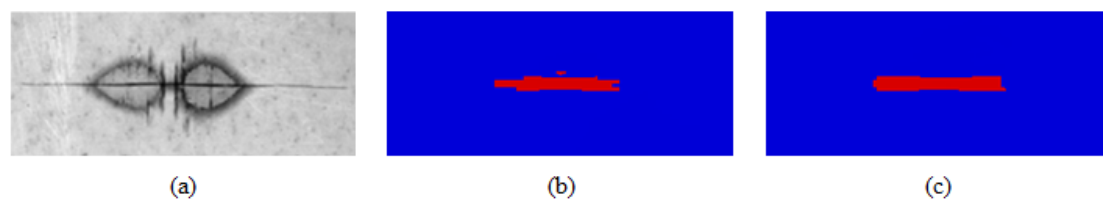


Figure 6. Comparison of matrix cracking in the bottom 0° plies (impact energy 2.1 J): (a) Experiment [5], (b) Prediction with shear non-linearity, and (c) Prediction without shear non-linearity.

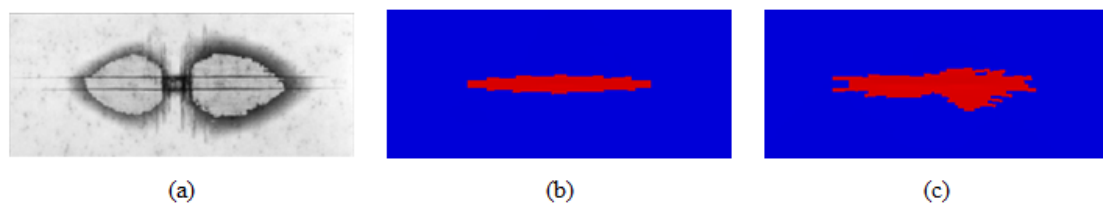


Figure 7. Comparison of matrix cracking in the bottom 0° plies (impact energy 5.1 J): (a) Experiment [5], (b) Prediction with shear non-linearity, and (c) Prediction without shear non-linearity.

sive failure and interlaminar delamination are considered in this model. Continuum shell elements with Hashin failure criteria and energy-based linear softening are employed to model in-plane behavior of composite plies, and cohesive elements with bilinear traction-separation laws are used to model the potential delamination between plies with different orientations. Non-linear in-plane shear behavior is also included by assuming a cubic stress-strain curve before damage initiation. Numerical simulations show that the proposed progressive damage model can accurately predict the dynamic response and damage patterns compared with experimental results from literature. By performing additional FE analyses without in-plane shear non-linearity, it is also found that it is necessary to include the non-linear in-plane

shear behavior for composite plies in order to predict accurate impact response.

Acknowledgments

The financial support from A*STAR is gratefully acknowledged and special thanks to professor Francesco Aymerich for providing the experimental data.

References

- [1] F. Aymerich, C. Pani, and P. Priolo. Damage response of stitched cross-ply laminates under impact loadings. *Engineering Fracture Mechanics*, 74(4):500–514, 2007.
- [2] M.V. Donadon, L. Iannucci, B.G. Falzon, J.M. Hodgkinson, and S.F.M. de Almeida. A progressive failure model for composite laminates subjected to low velocity impact damage. *Computers & Structures*, 86(11-12):1232–1252, 2008.
- [3] F. Aymerich and P. Priolo. Characterization of fracture modes in stitched and unstitched cross-ply laminates subjected to low-velocity impact and compression after impact loading. *International Journal of Impact Engineering*, 35(7):591–608, 2008.
- [4] C. Bouvet, S. Rivallant, and J.J. Barrau. Low velocity impact modeling in composite laminates capturing permanent indentation. *Composites Science and Technology*, 72(16):1977–1988, 2012.
- [5] F. Aymerich, F. Dore, and P. Priolo. Prediction of impact-induced delamination in cross-ply composite laminates using cohesive interface elements. *Composites Science and Technology*, 68(12, SI):2383–2390, 2008.
- [6] F. Aymerich, F. Dore, and P. Priolo. Simulation of multiple delaminations in impacted cross-ply laminates using a finite element model based on cohesive interface elements. *Composites Science and Technology*, 69(11-12):1699–1709, 2009.
- [7] D. Feng and F. Aymerich. Finite element modelling of damage induced by low-velocity impact on composite laminates. *Composite Structures*, 108:161–171, 2014.
- [8] Z.C. Su, T.E. Tay, M. Ridha, and B.Y. Chen. Progressive damage modeling of open-hole composite laminates under compression. *Composite Structures*, 122:507–517, 2015.
- [9] Z. Hashin. Failure criteria for unidirectional fiber composites. *Journal of Applied Mechanics-Transactions ASME*, 47(2):329–334, 1980.
- [10] S.T. Pinho, L. Iannucci, and P. Robinson. Physically-based failure models and criteria for laminated fibre-reinforced composites with emphasis on fibre kinking: Part I: Development. *Composites Part A-Applied Science and Manufacturing*, 37(1):63–73, 2006.
- [11] S.T. Pinho, L. Iannucci, and P. Robinson. Physically based failure models and criteria for laminated fibre-reinforced composites with emphasis on fibre kinking. Part II: FE implementation. *Composites Part A-Applied Science and Manufacturing*, 37(5):766–777, 2006.
- [12] Dassault Systèmes Simulia Corp. *Abaqus Analysis User's Manual, Version 6.10*, 2010.
- [13] R.D.S.G Campilho, M.F.S.F. de Moura, and J.J.M.S. Domingues. Modelling single and double-lap repairs on composite materials. *Composites Science and Technology*, 65(13):1948 – 1958, 2005.